APPENDIX A

This appendix contains a review of the fractographic work presented in the AREVA report. “Shell C, Fractographic Investigation of fracture faces – Material 1.2MD07. D02-ARV-01-086-123 Rev. A.” AXPO 2015.

Table 1: Summmary of fractographic results given in D02-ARV-01-086-123 Rev. A: CF = Cleavage Fracture, FC = Fatigue Crack, T = Transition between fatigue crack and cleavage fracture [1].

	Sample No.	Sample Orientation	Characteristics	Location	Dimension	Appendix
Fig. A1	C28	Charpy V-notch; L-T	local nonmetallic inclusions	CF	approx. 30 µm	1 (irradiated)
			ductile area on fracture face	CF	approx. 2 mm	
Fig. A2	C7C	reconstituted SE(B) 10x10x55 specimen reconstituted specimen;T-L	MnS inclusions	CF and T	approx. 170 µm – 700 µm	
			intergranular features	FC	about 100 µm	
Fig. A3	C8C	reconstituted SE(B) 10x10x55 specimen reconstituted specimen;T-L	MnS inclusions	FC and T	< 100 µm	
			intergranular features	FC	about 100 µm	
Fig. A4	C27L	Charpy V-notch; L-T	ductile areas on fracture face	CF	about 100 µm	
Fig. A5	C8B	reconstituted SE(B) 10x10x55 specimen reconstituted specimen;T-L	intergranular features	FC	about 100 µm	
Fig. A6	C23R	reconstituted SE(B) 10x10x55 specimen; L-T	intergranular features	CF and FC	about 100 µm	
			MnS inclusions	CF	< 50 µm	
Fig. A7	C26R	reconstituted SE(B) 10x10x55 specimen; L-T	intergranular features	FC	about 100 µm	
			MnS inclusions	CF and FC	< 50 µm	
Fig. A8	C22L	reconstituted SE(B) 10x10x55 specimen; L-T	intergranular features	FC	about 100 µm	
			MnS inclusions	CF	< 100 µm	
Fig. A9	C8	WOL-25X; T-L	intergranular features	FC	about 100 µm	
			ductile area of fracture face	CF	approx. 260 µm x 400 µm	
			MnS inclusions	FC	approx. 50 µm – 100 µm	
			MnS inclusions	CF	approx. 150 µm	
Fig. A10	B1C.3	CT-25; T-L	MnS inclusions	CF	approx. 300 µm	2 (unirradiated)
			Al_2O_3 inclusions	CF, FC and T	isolated inclusions: approx. 10 µm inclusion lines: < 150 µm	
Fig. A11	B1C.5	CT-25; T-L	MnS inclusions	end of CF	approx. 500 µm	
			Al_2O_3 inclusions	FC	approx. 250 µm	
Fig. A12	B1C.7	CT25; T-L	MnS inclusions	end of CF	approx. 500 µm – 1 3 mm	
			intergranular features	FC and T	about 100 µm	
			Al_2O_3 inclusions	FC	approx. 85 µm	
Fig. A13	B1C.1.2	CT10; T-L	MnS inclusions	end of CF and T	approx. 400 µm – 600 µm	
			Al_2O_3 inclusions	FC	isolated inclusions: approx. 10 µm inclusion lines: < 250 µm	
Fig. A14	B1C.2.2	CT10; T-L	Al_2O_3 inclusions	CF	approx. 10 µm	
Fig. A15	B1C.3.1	CT10; T-L	Al_2O_3 inclusions	FC	isolated inclusions: approx. 10 µm inclusion lines: < 200 µm	
Fig. A16	B1C.R2.6	SE(B) 10x10x55 specimen; T-L	Al_2O_3 inclusions	FC	isolated inclusions: approx. 10 µm inclusion line: approx. 200 µm	
Fig. A17	B1C.9.6	SE(B) 10x10x55 specimen; T-L	-	-	-	
Fig. A18	B1C.9.9	SE(B) 10x10x55 specimen; T-L	Al_2O_3 inclusion	CF	approx. 100 µm	
Fig. A19	B1C9.11	SE(B) 10x10x55 specimen; T-L	-	-	-	

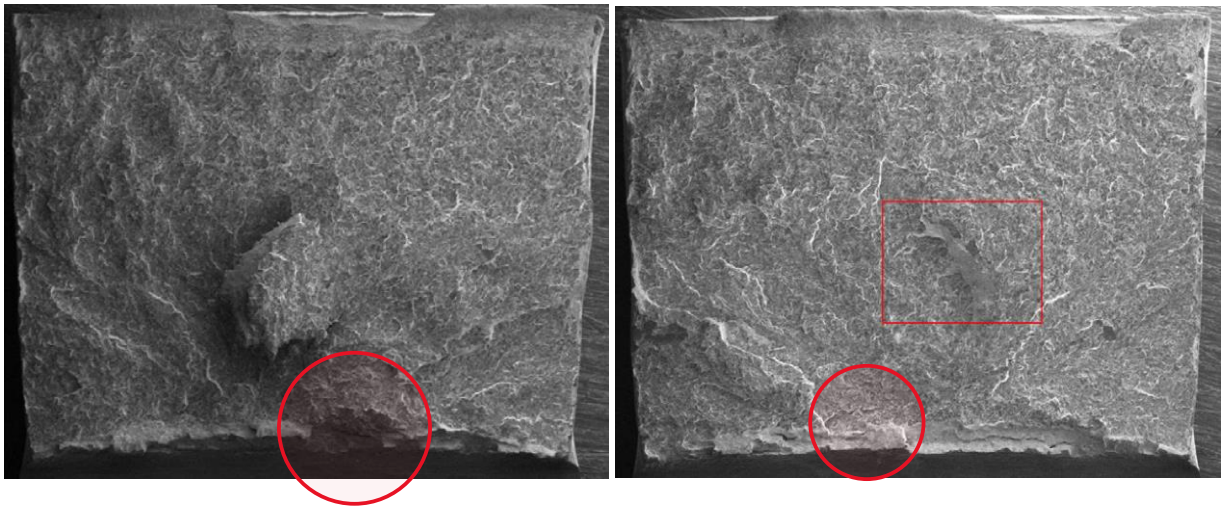

Figure A1. Left and right fracture surface of irradiated Charpy-V specimen C28, showing predominantly cleavage fracture. There is a short region of ductile tearing, prior to cleavage, at the notch root. The primary cleavage fracture initiation region is marked by a red circle. The fracture surface is rough and due to different fracture planes, a region close to the center of the specimen, has fractured by shear, resulting in ductile fracture. This ductile fracture is due to crack plane mis-orientation and is not an indication of low upper shelf toughness. Cleavage initiation is in a region without special features.

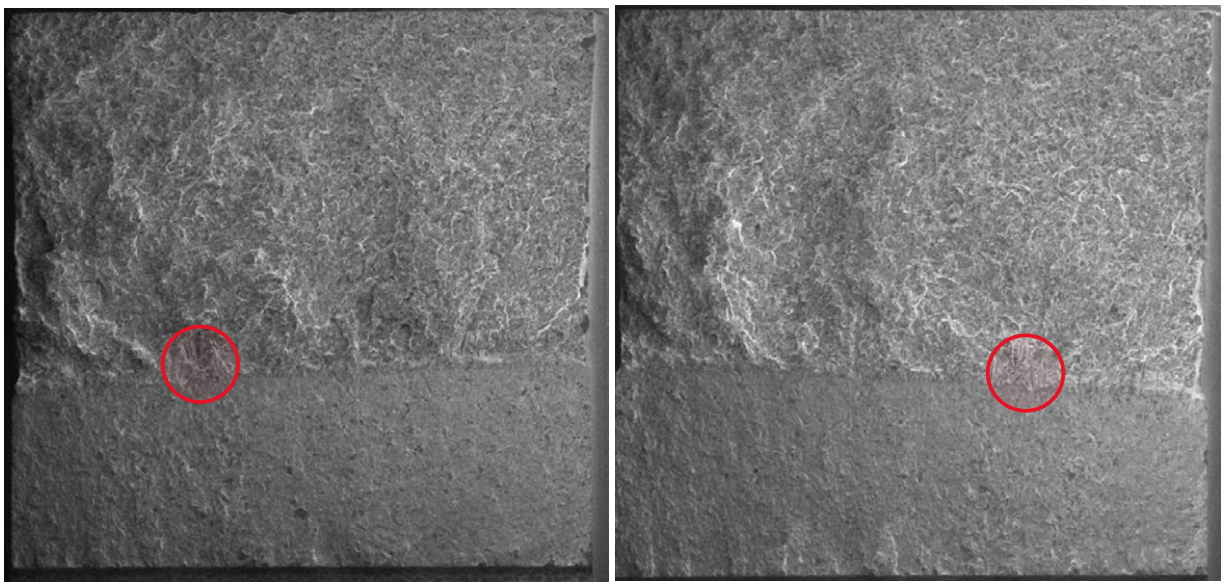

Figure A2. Left and right fracture surface of irradiated SE(B) specimen C7C, manufactured from a WOL specimen, showing predominantly cleavage fracture. The specimen was tested at 30°C and the fracture toughness was K_{Jc} = 158 MPa√m. The primary cleavage fracture initiation region is marked by a red circle. The fracture surface contains MnS inclusions located at the fatigue crack tip and some located in front of the crack in the cleavage fracture region. Primary cleavage initiation may be connected to MnS inclusions The fatigue surface contains patches of intergranular fracture, but intergranular fracture is not visible in the cleavage fracture region.

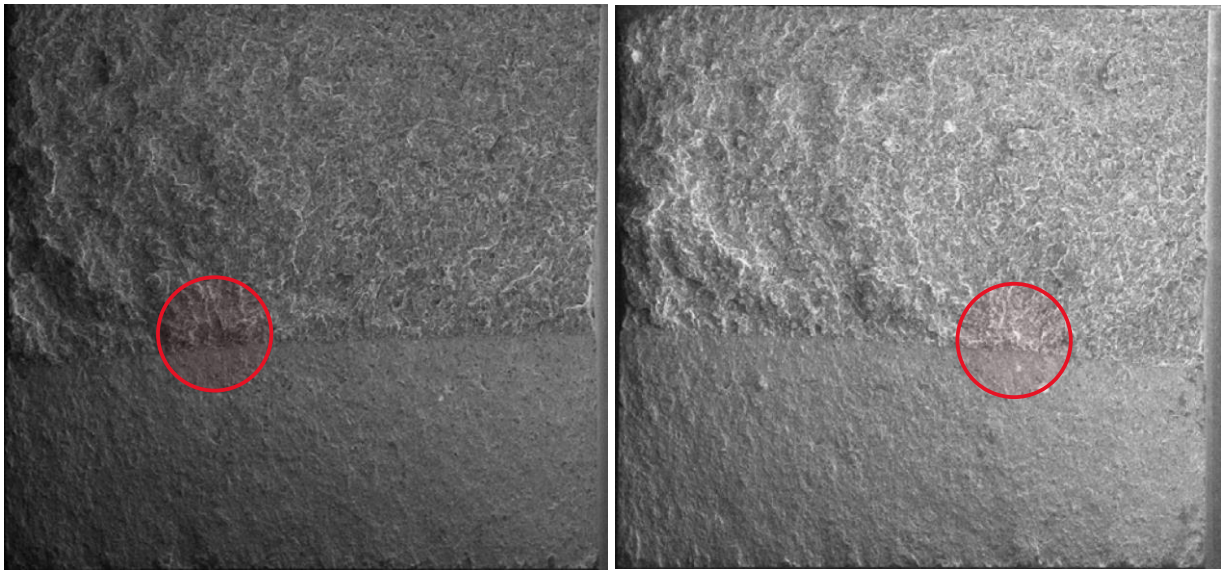

Figure A3. Left and right fracture surface of irradiated SE(B) specimen C8C, manufactured from a WOL specimen, showing predominantly cleavage fracture. The specimen was tested at 25°C and the fracture toughness was K_{Jc} = 71 MPaVm. The primary cleavage fracture initiation region is marked by a red circle. The fracture surface contains some MnS inclusions located close to the fatigue crack tip, but primary cleavage initiation does not seem to be connected to MnS inclusions The fatigue surface contains patches of intergranular fracture, but intergranular fracture is not visible in the cleavage fracture region.

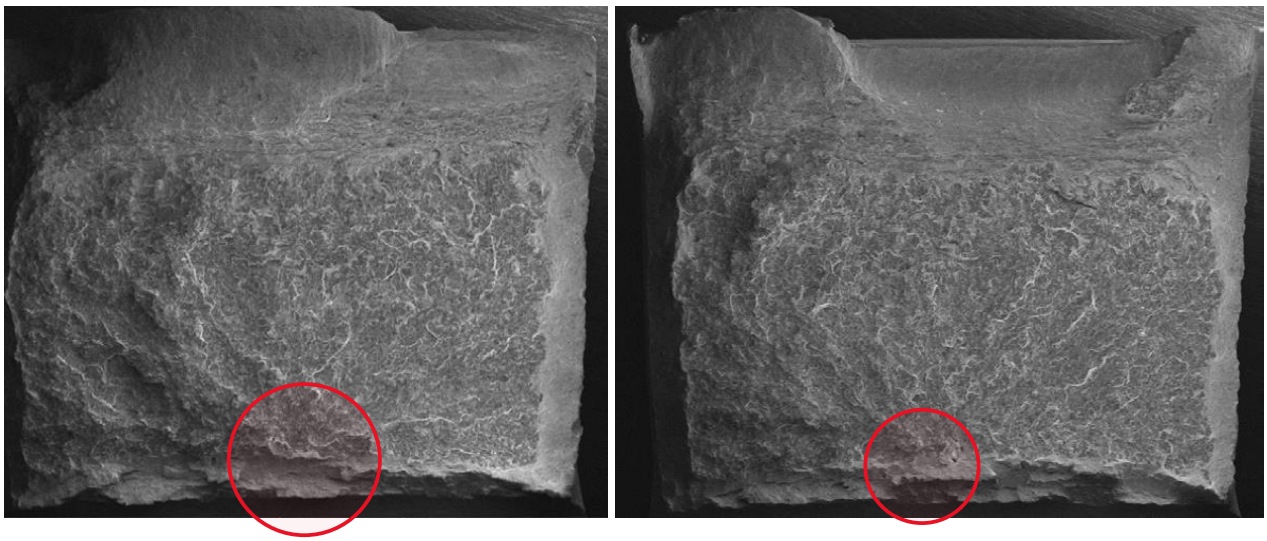

Figure A4. Left and right fracture surface of irradiated Charpy-V specimen C27L, showing predominantly cleavage fracture. There is a region of ductile tearing, prior to cleavage, at the notch root. The primary cleavage fracture initiation region is marked by a red circle. Based on the heavy deformation of the specimen, the impact energy of the test must be quite high. The fracture surface is very rough and due to different fracture planes, several regions have fractured by shear, resulting in ductile fracture. This ductile fracture is due to crack plane mis-orientation and is connected to the high impact energy.

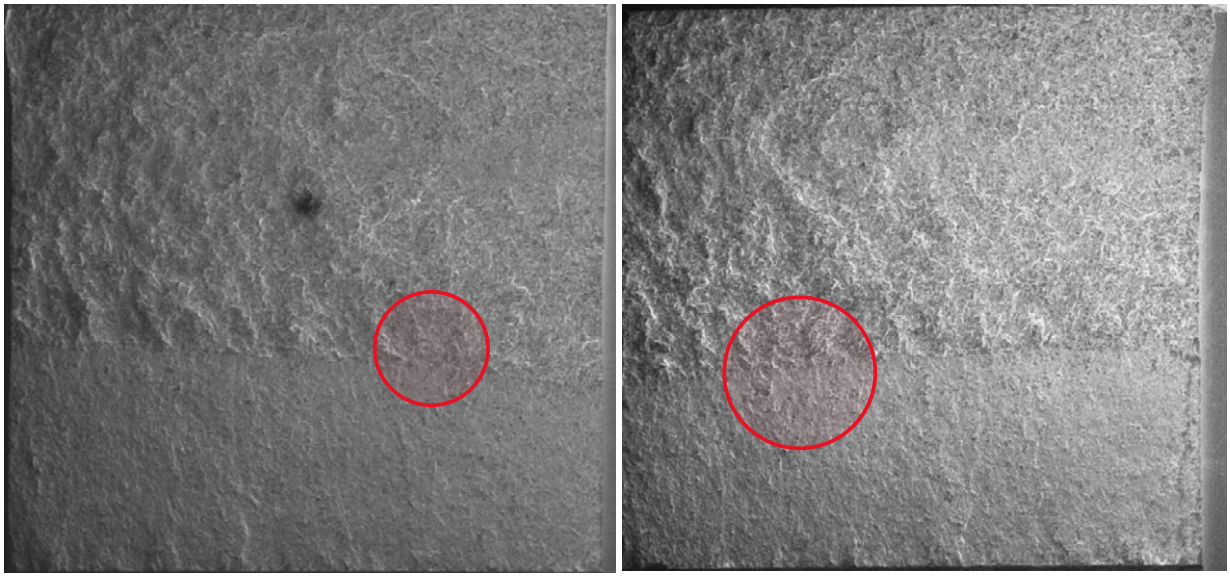

Figure A5. Left and right fracture surface of irradiated SE(B) specimen C8B, manufactured from a WOL specimen, showing cleavage fracture. The specimen was tested at 15°C and the fracture toughness was K_{Jc} = 48 MPa√m. The primary cleavage fracture initiation region is marked by a red circle. The cleavage fracture region is quite flat, which limits the amount of shear fracture betwee n different fracture planes. The fatigue surface contains patches of intergranular fracture, but intergranular fracture is not visible in the cleavage fracture region. Fatigue crack growth is controlled by a strain accumulation mechanism, and this makes fatigue crack growth more sensitive to grain boundary fracture. Cleavage initiation occurs in a region without special features.

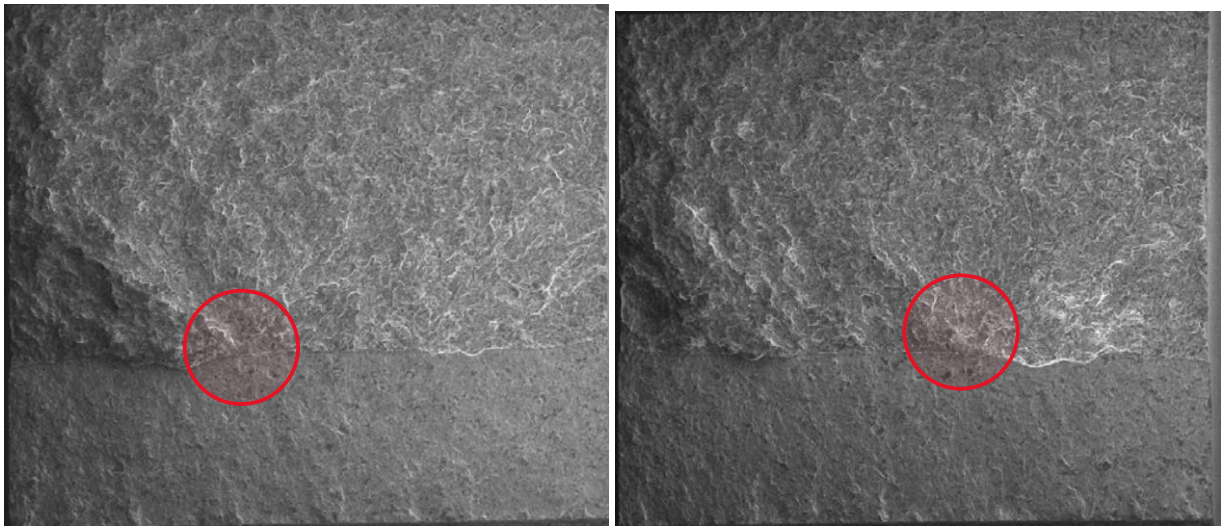

Figure A6. Left and right fracture surface of irradiated SE(B) specimen C23R, manufactured from a CVN specimen, showing predominantly cleavage fracture. The primary cleavage fracture initiation region is marked by a red circle. The surface roughness indicates a K_{Jc} value around 100 MPa√m. The fatigue surface contains patches of intergranular fracture, but intergranular fracture is not visible in the cleavage fracture region. Fatigue crack growth is controlled by a strain accumulation mechanism, and this makes fatigue crack growth more sensitive to grain boundary fracture. Cleavage initiation occurs in a region without special features, but there are isolated regions of grain boundary fracture in the cleavage region. This indicates some grain boundary segregation, but grain boundary fracture did not affect the cleavage

initiation, being a secondary event. Manganese sulfides present among the cleavage fracture region did not affect the cleavage initiation.

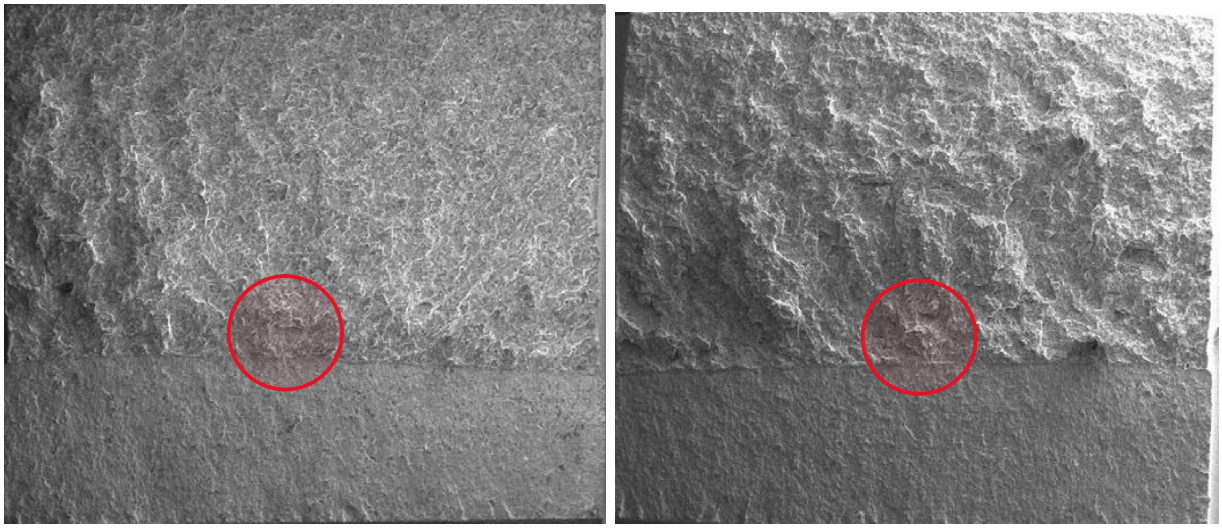

Figure A7. Left and right fracture surface of irradiated SE(B) specimen C26R, manufactured from a CVN specimen, showing predominantly cleavage fracture. The primary cleavage fracture initiation region is marked by a red circle. The surface roughness indicates a K_{Jc} value above 100 MPa√m. The fatigue surface contains patches of intergranular fracture, but intergranular fracture is not visible in the cleavage fracture region. Fatigue crack growth is controlled by a strain accumulation mechanism, and this makes fatigue crack growth more sensitive to grain boundary fracture. Cleavage initiation occurs in a region without special features. Manganese sulfides present among the cleavage fracture region did not affect the cleavage initiation.

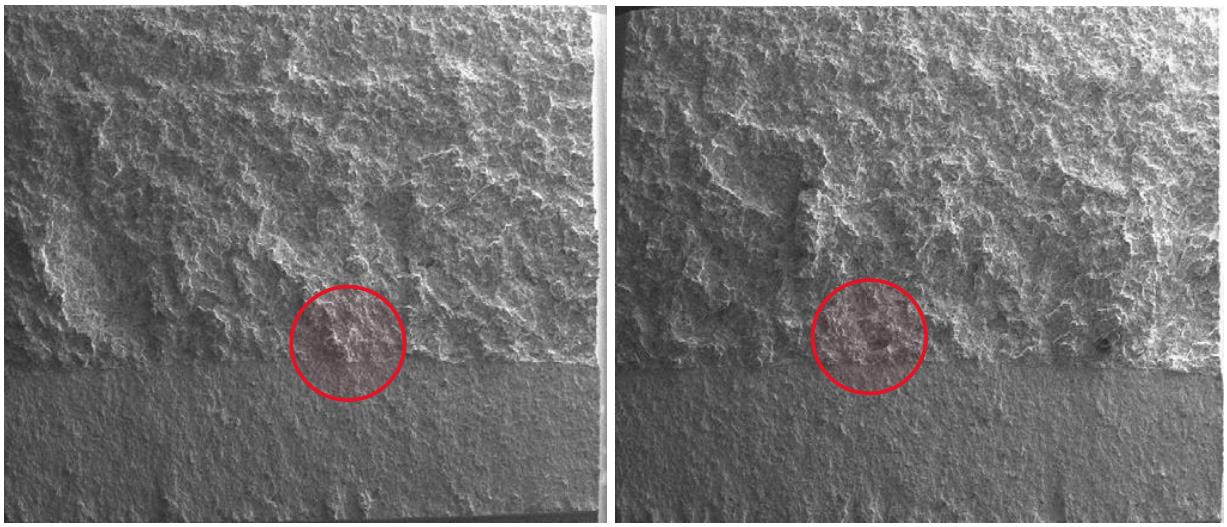

Figure A8. Left and right fracture surface of irradiated SE(B) specimen C22L, manufactured from a CVN specimen, showing predominantly cleavage fracture. The approximate primary cleavage fracture initiation region is marked by a red circle. The surface roughness indicates a K_{Jc} value around 100 MPa√m. The fatigue surface contains some patches of intergranular fracture, but intergranular fracture is not visible in the cleavage fracture region. Fatigue crack growth is controlled by a strain accumulation mechanism, and this makes fatigue crack growth more sensitive to grain boundary fracture. Cleavage initiation occurs in a region

without special features. Manganese sulfides present among the cleavage fracture region did not appear to affect the cleavage initiation.

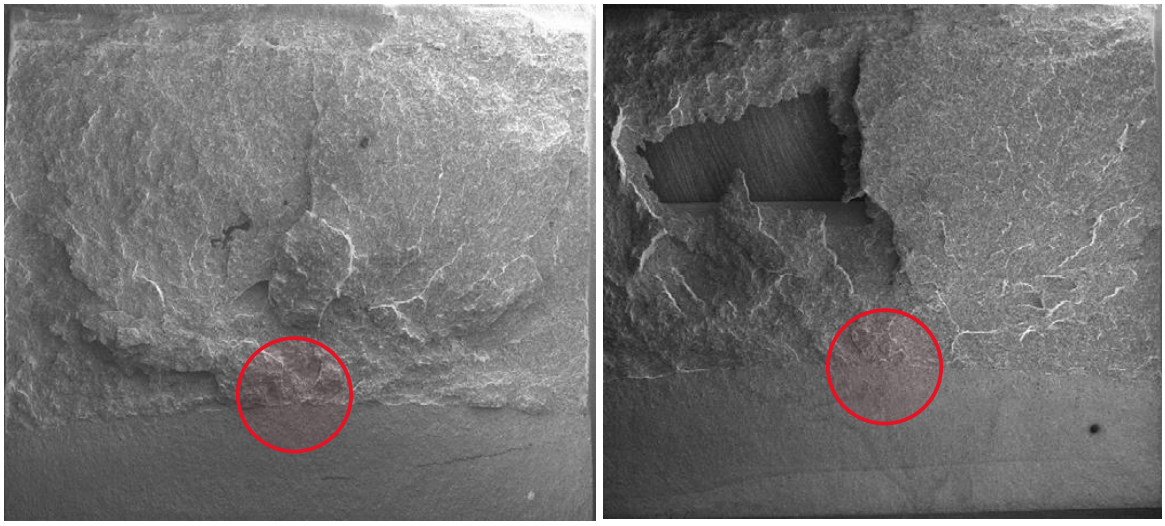

Figure A9. Left and right fracture surface of irradiated 25 mm WOL specimen C8, showing predominantly cleavage fracture. The primary cleavage fracture initiation region is marked by a red circle. The surface roughness indicates a K_{Jc} value above 100 MPa√m. The fatigue surface contains patches of intergranular fracture, but intergranular fracture is not visible in the cleavage fracture initiation region. Fatigue crack growth is controlled by a strain accumulation mechanism, and this makes fatigue crack growth more sensitive to grain boundary fracture. Cleavage initiation occurs in a region without special features, but there are isolated regions of grain boundary fracture in the cleavage region. This indicates some grain boundary segregation, but grain boundary fracture did not affect the cleavage initiation, being a secondary event. Manganese sulfides present among the cleavage fracture region did not appear to affect the cleavage initiation. Small patches of ductile fracture appear to be secondary events due to deviations in the cleavage fracture planes.

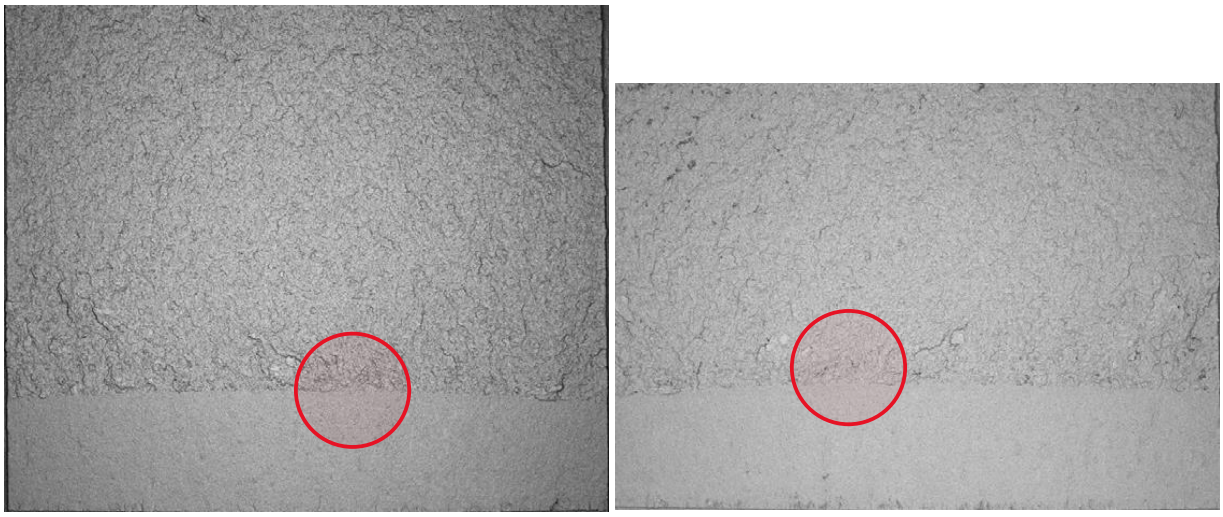

Figure A10. Left and right fracture surface of unirradiated 25 mm C(T) specimen B1C.3, showing predominantly cleavage fracture. The primary cleavage fracture initiation region is marked by a red circle. The test temperature was -70°C and the fracture toughness 49.3 MPa√m which explains the flatness of the fracture surface. Cleavage initiation occurs in a region without special features, but there are isolated Al_2O_3

inclusions located both in the fatigue crack growth region, cleavage fracture region and on the fatigue crack front. Because cleavage fracture initiation generally occur some distance in front of the fatigue crack, these inclusions are unlikely to have caused cleavage fracture initiation. However, since the location of the Al_2O_3 inclusions with respect to the initiation site is not known, an interaction of the inclusions cannot be ruled out. Manganese sulfides present among the cleavage fracture region did not appear to affect the cleavage initiation. Small patches of ductile fracture appear to be secondary events due to deviations in the cleavage fracture planes.

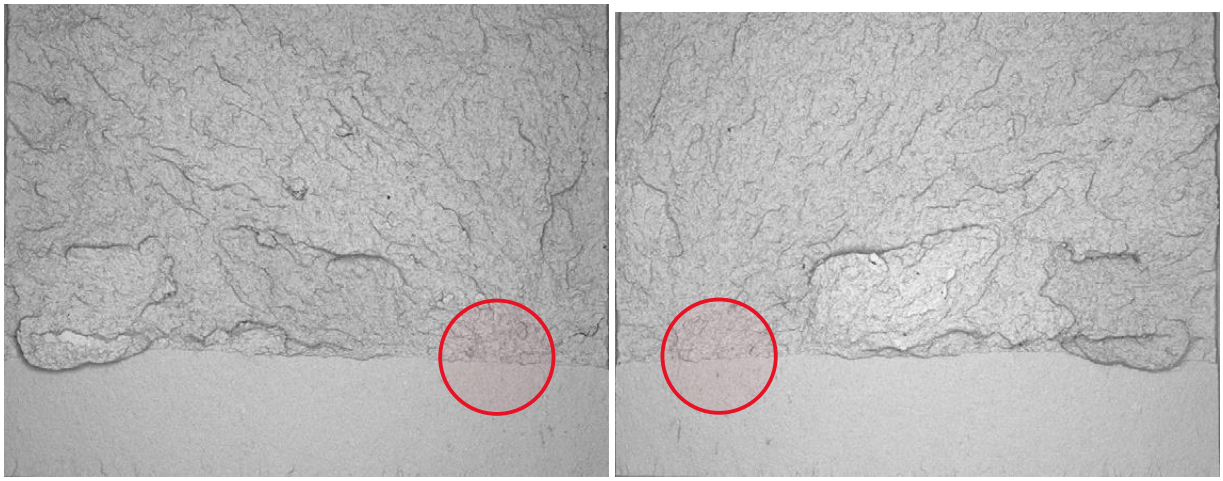

Figure A11. Left and right fracture surface of unirradiated 25 mm C(T) specimen B1C.5, showing predominantly cleavage fracture. The primary cleavage fracture initiation region is marked by a red circle. The test temperature was +5°C and the fracture toughness 111.8 MPa√m which explains the larger roughness of the fracture surface. Cleavage initiation occurs in a region without special features. There are isolated Al_2O_3 inclusions located in the fatigue crack growth region, but none are identified in the cleavage fracture region. Manganese sulfides present close to the end of the specimen are unrelated to cleavage fracture initiation.

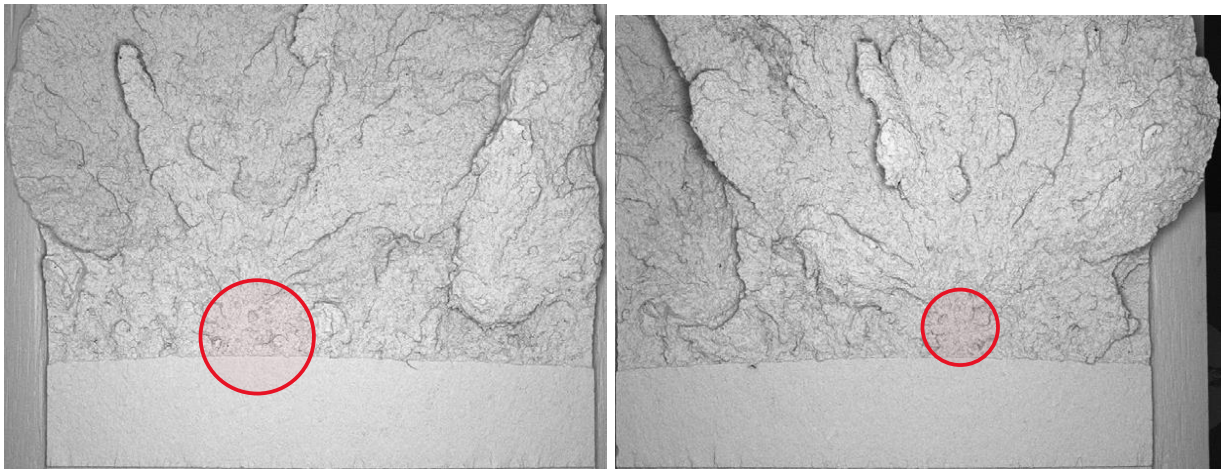

Figure A12. Left and right fracture surface of unirradiated 25 mm C(T) specimen B1C.7, showing predominantly cleavage fracture. The primary cleavage fracture initiation region is marked by a red circle. The test temperature was -30°C and the fracture toughness 148.1 MPa√m which explains the considerable roughness of the fracture surface. Cleavage initiation occurs in a region without special features. There are isolated Al_2O_3 inclusions located in the fatigue crack growth region, but none are identified in the cleavage fracture region. Manganese sulfides present close to the end of the specimen are unrelated to cleavage

fracture and manganese sulfides close to the fatigue crack tip are too far from the cleavage initiation site. Some local grain boundary fracture details are found in the fatigue region, but they are not connected to the cleavage fracture initiation.

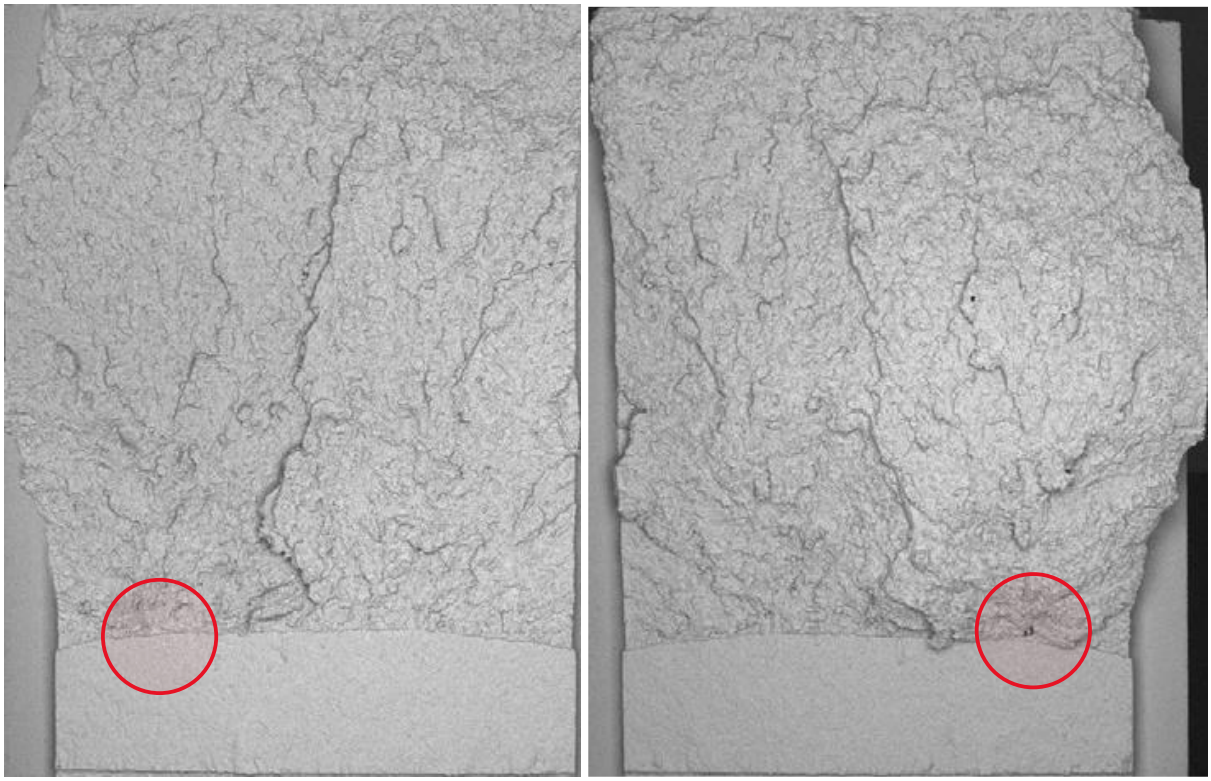

Figure A13. Left and right fracture surface of unirradiated 10 mm C(T) specimen B1C.1.2, showing predominantly cleavage fracture. The primary cleavage fracture initiation region is marked by a red circle. The test temperature was -85°C and the fracture toughness 138.4 MPa√m which explains the considerable roughness of the fracture surface. Cleavage initiation occurs in a region without special features. There are isolated Al_2O_3 inclusions located in the fatigue crack growth region, but none are identified in the cleavage fracture region. Manganese sulfides present close to the end of the specimen are unrelated to cleavage fracture. Manganese sulfides at the fatigue crack tip can possibly have interacted with the cleavage fracture if they are close to the initiation site. Their location information is, however, not given.

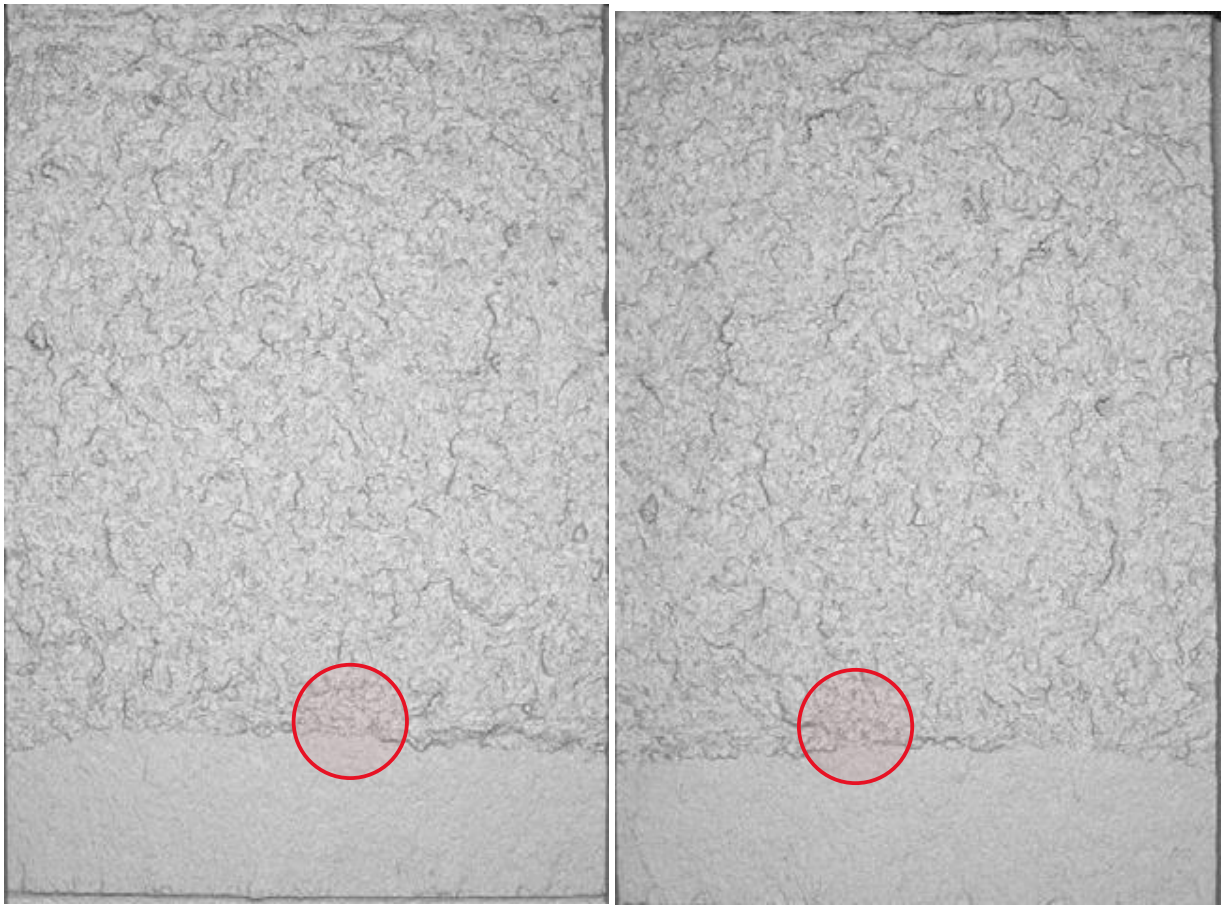

Figure A14. Left and right fracture surface of unirradiated 10 mm C(T) specimen B1C.2.2, showing predominantly cleavage fracture. The likely primary cleavage fracture initiation region is marked by a red circle. The test temperature was -85°C and the fracture toughness 37.1 MPa√m which explains the flatness of the fracture surface. Cleavage initiation occurs in a region without special features. There are isolated Al_2O_3 inclusions located in the cleavage fracture region, but they are not connected to the cleavage initiation event.

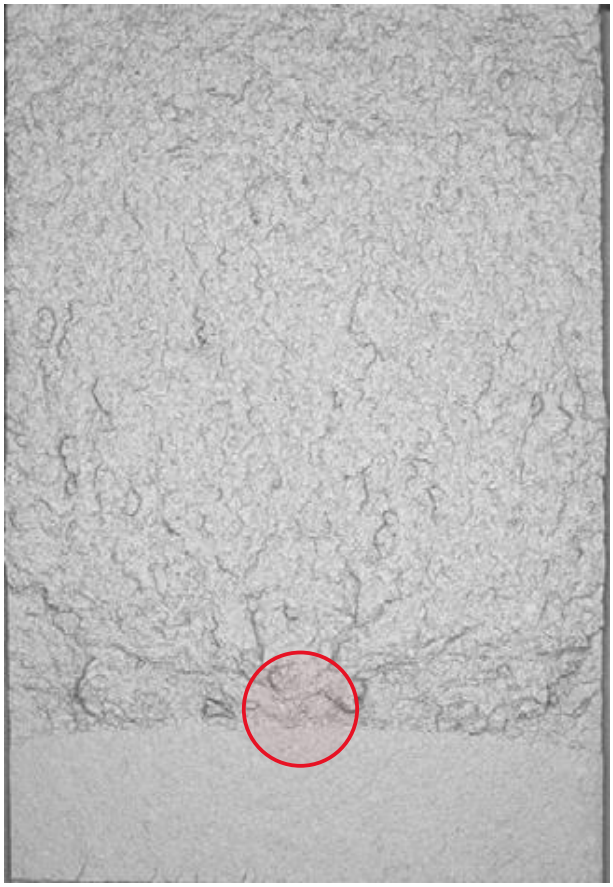

Figure A15. Left fracture surface of unirradiated 10 mm C(T) specimen B1C.3.1, showing predominantly cleavage fracture. The likely primary cleavage fracture initiation region is marked by a red circle. The test temperature was -105°C and the fracture toughness 59.6 MPa√m. Cleavage initiation occurs in a region without special features. There are isolated Al_2O_3 inclusions located in the fatigue fracture region, but they are not connected to the cleavage initiation event.

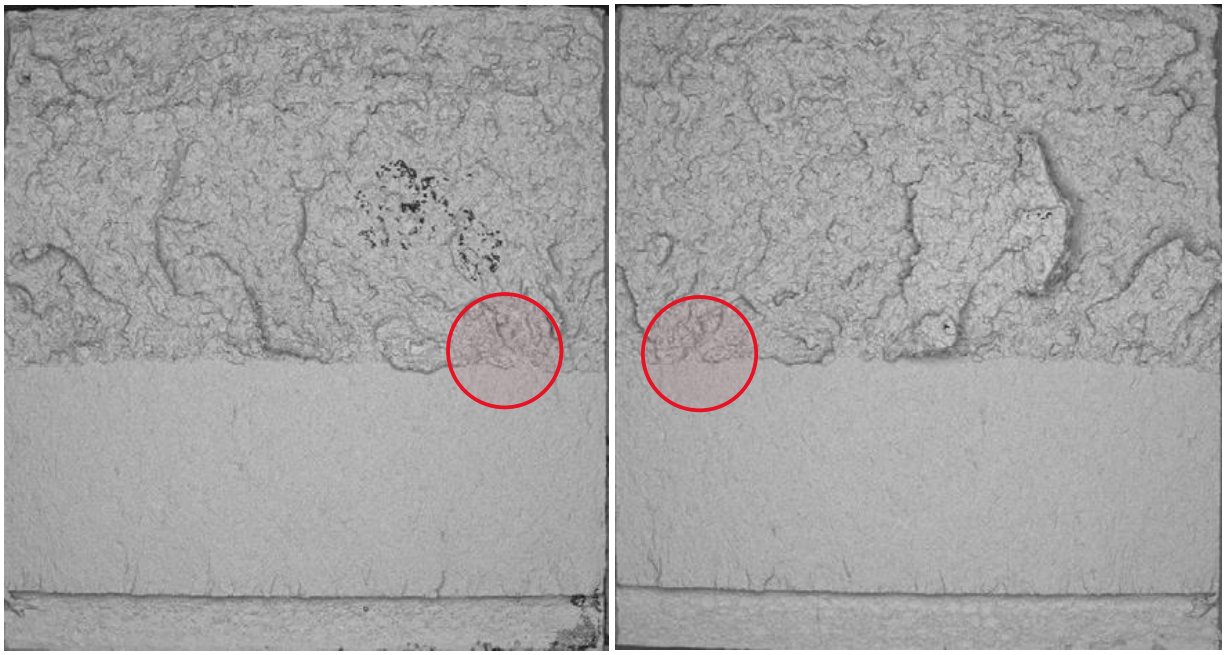

Figure A16. Left and right fracture surface of unirradiated SE(B) specimen B1C.R2.6, showing predominantly cleavage fracture. The approximate primary cleavage fracture initiation region is marked by a red circle. The test temperature was -90°C and the fracture toughness 73.6 MPa√m. Cleavage initiation occurs in a region without special features. There are isolated Al_2O_3 inclusions located in the fatigue fracture region, but they are not connected to the cleavage initiation event. Manganese sulfides at the fatigue crack tip can possibly have interacted with the cleavage fracture if they are close to the initiation site. Their location information is, however, not given.

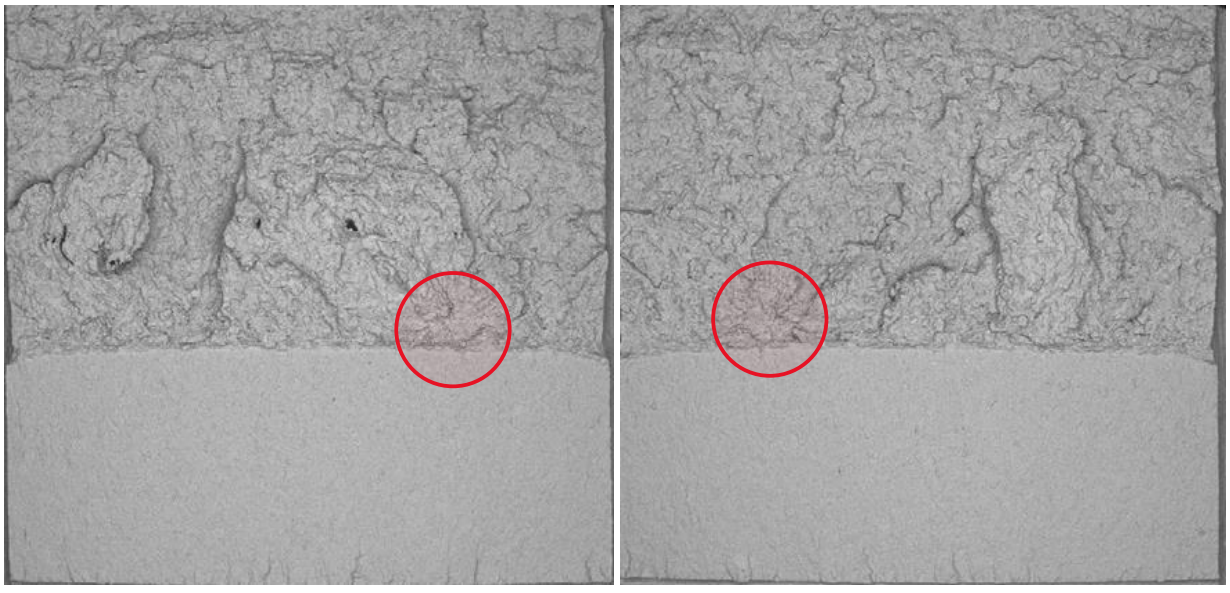

Figure A17. Left and right fracture surface of unirradiated SE(B) specimen B1C.9.6, showing predominantly cleavage fracture. The approximate primary cleavage fracture initiation region is marked by a red circle. The test temperature was -90°C and the fracture toughness was rather high 198.8 MPa√m and the initiation site lies quite far from the fatigue crack tip. Cleavage initiation occurs in a region without special features. No finding related to inclusions are reported.

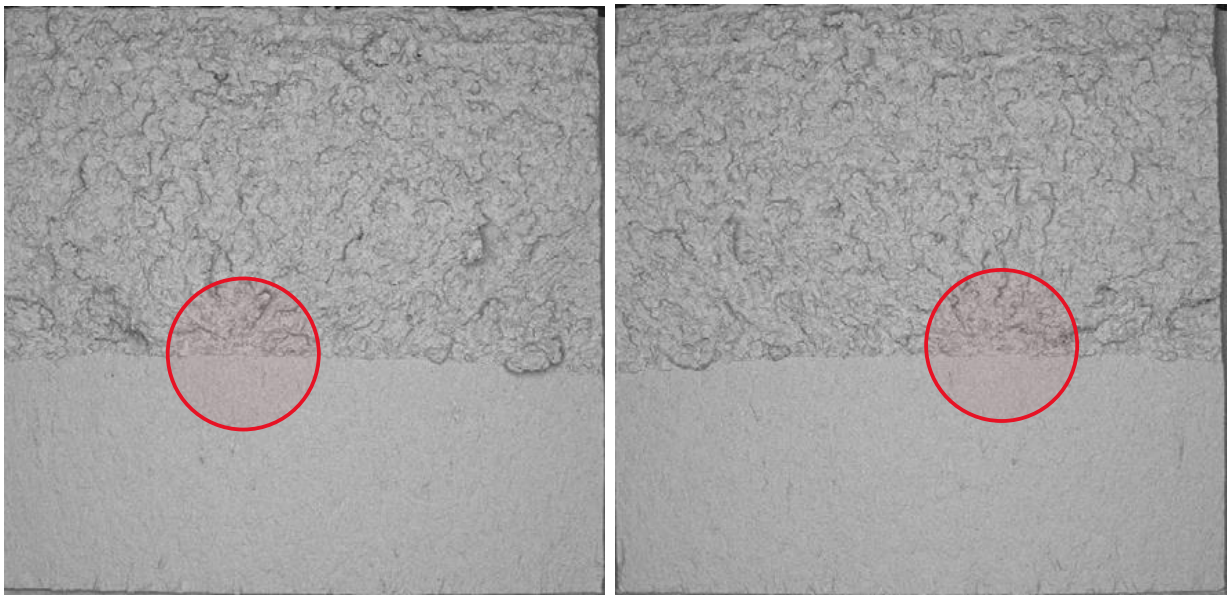

Figure A18. Left and right fracture surface of unirradiated SE(B) specimen B1C.9.9, showing predominantly cleavage fracture. The approximate primary cleavage fracture initiation region is marked by a red circle. The test temperature was -85°C and the fracture toughness was 79.2 MPa√m. Cleavage initiation occurs in a region without special features. Al_2O_3 inclusions were reported close to the side of the specimen and MnS inclusions were found on the fatigue surface. Neither are connected to the cleavage initiation of the specimen.

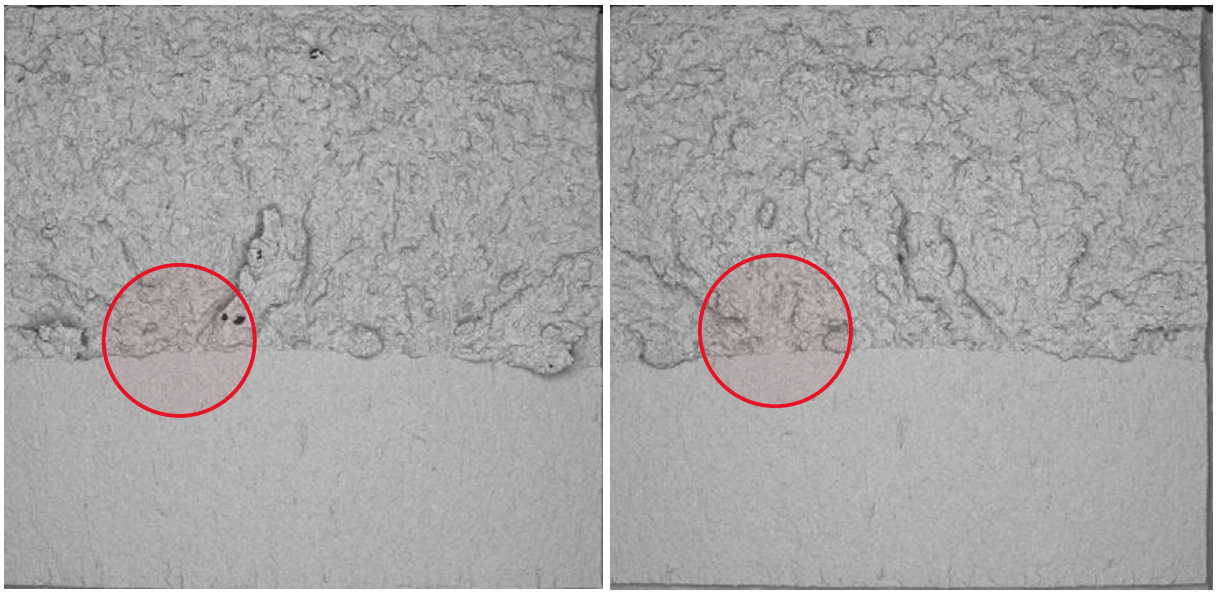

Figure A19. Left and right fracture surface of unirradiated SE(B) specimen B1C.9.11, showing predominantly cleavage fracture. The approximate primary cleavage fracture initiation region is marked by a red circle. The test temperature was -80°C and the fracture toughness was 84.3 MPa√m. Cleavage initiation occurs in a region without special features. No finding related to inclusions are reported.